Published in final edited form as:
Nat Struct Mol Biol. 2012 October ; 19(10): 1018–1022. doi:10.1038/nsmb.2376.

A bi-phasic pulling force acts on transmembrane helices during translocon-mediated membrane integration

Nurzian Ismail[1], **Rickard Hedman**[1], **Nina Schiller**[1], and **Gunnar von Heijne**[1,2,#]

[1]Center for Biomembrane Research, Department of Biochemistry and Biophysics, Stockholm University, SE-106 91 Stockholm, Sweden

[2]Science for Life Laboratory Stockholm University, Box 1031, SE-171 21 Solna, Sweden

Abstract

Membrane proteins destined for insertion into the inner membrane of bacteria or the endoplasmic reticulum membrane in eukaryotic cells are synthesized by ribosomes bound to the bacterial SecYEG or the homologous eukaryotic Sec61 translocon. During co-translational membrane integration, transmembrane α-helical segments in the nascent chain exit the translocon via a lateral gate that opens towards the surrounding membrane, but the mechanism of lateral exit is not well understood. In particular, little is known about how a transmembrane helix behaves when entering and exiting the translocon. Using translation-arrest peptides from bacterial SecM proteins and from the mammalian Xbp1 protein as force sensors, we show that substantial force is exerted on a transmembrane helix at two distinct points during its transit through the translocon channel, providing direct insight into the dynamics of membrane integration.

Keywords

membrane protein; Sec translocon; SecM, Xbp1, translation arrest; transmembrane helix; membrane integration

In both prokaryotic and eukaryotic cells, most membrane proteins are co-translationally inserted into the membrane with the aid of Sec-type translocons [1]. While the energetics of membrane insertion is now rather well understood [2-4], dynamic aspects have received little attention. We reasoned that direct dynamic information on the insertion process might be obtained if local forces acting on a hydrophobic segment in the nascent polypeptide chain could be measured as a function of the segment's location in the ribosome-translocon complex. To detect such forces during co-translational integration of membrane proteins into the inner membrane of *Escherichia coli* and the mammalian endoplasmic reticulum (ER) membrane, we decided to explore the possible utility of so-called translation-arrest peptides [5] as natural force sensors.

Arrest peptides have been identified both in prokaryotic and eukaryotic proteins. SecM is a prokaryotic periplasmic protein harboring an arrest peptide that helps regulate the expression of the co-transcribed translocation-motor protein SecA [6]. During translation of SecM, the arrest peptide causes efficient ribosome stalling by blocking the incorporation of a critical proline residue into the elongating nascent chain [7]. There is strong support for the idea that

[#]Corresponding author. Phone: Int+46-8-16 25 90. Fax: Int+46-8-15 36 79. gunnar@dbb.su.se.

Author contributions

N.I., R.H., and N.S. contributed to the study design, the experimental work, and the writing of the paper. G.v.H contributed to the study design and the writing of the paper.

Europe PMC Funders Author Manuscripts

stalling is prevented if an external “pulling force” is exerted on the nascent chain at the precise point when the ribosome reaches the critical proline residue at end of the arrest peptide [7-13]. During SecYEG-mediated translocation of SecM into the periplasm, the pulling force needed to overcome the translational arrest and reactivate peptide bond formation at the peptidyl transferase center is thought to be supplied by SecA [7].

We hypothesized that an additional pulling force might be generated when a hydrophobic segment transits through the translocon, since membrane integration of transmembrane helices is driven by a substantial free-energy gradient between the translocon channel and the surrounding membrane [3,14]. To detect such a force, we engineered two different SecM arrest peptides into a model inner membrane protein and studied the constructs by pulse-chase analysis in live *Escherichia coli* cells. Additionally, we analyzed similar constructs incorporating the mammalian Xbp1 arrest peptide [15] by *in vitro* translation in the presence of dog pancreas rough microsomes.

Results

The Lep-SecM model system

We first introduced the shortest known arrest peptide, the eight-residue sequence HAPIRGSP from *Mannheimia succiniciproducens* (*Ms*) SecM [16], as well as the related, 17-residue arrest peptide FSTPVWISQAQGIRAGP from *E. coli* (*Ec*) SecM [17], near the C terminus of leader peptidase (Lep), a well-characterized *E. coli* inner membrane protein with two N-terminal transmembrane α-helices (TM1, TM2) and a large C-terminal periplasmic domain [18], Figure 1a. In addition, we placed 19-residue long leucine-alanine based segments of varying hydrophobicity (H segments; see Supplementary Tables 1 and 2 for sequences of H segments and arrest peptides) flanked by GGPG…GPGG tetrapeptides [2] in the C-terminal domain at different distances *L* upstream of the arrest peptide, with the expectation that a force exerted on the H segment at the point when the ribosome reaches the critical proline residue at end of the arrest peptide could be detected as an increase in the amount of full length Lep-SecM protein. By varying *L* and the composition of the H segment, we could analyze how the pulling force varies both with the location of the H segment in the ribosome–translocon-nascent chain conduit and with H-segment hydrophobicity. Membrane-insertion efficiencies into both the ER and the *E. coli* inner membrane have been measured previously for a large panel of H segments inserted into the Lep protein [2,3,14], allowing a direct comparison between insertion efficiency and pulling force.

As shown by the pulse-chase analysis in Figure 1b, the SecM(*Ms*) and the SecM(*Ec*) arrest peptides induce efficient translation arrest of the Lep-SecM constructs, and hence there is no detectable pulling force on the nascent chain, when the critical proline residue in the arrest peptides is located *L* = 63 or 72 residues downstream of a strongly hydrophobic, transmembrane [6L/13A] H segment. Presumably, this is because the transmembrane segment has already been integrated into the membrane at the time of arrest so that the C-terminal part of the protein is not pulled upon by SecA or other components of the translocation machinery, as suggested previously for a SecM construct where a transmembrane segment was placed 75 residues upstream of the arrest peptide [8]. When the two arrest peptides are inactivated by mutating the critical proline residue to alanine [11,16], only non-arrested, full length Lep-SecM chains are seen. Precipitation of the arrested form of Lep-SecM(*Ms*) with cetyltrimethylammonium bromide shows that the tRNA remains attached to the nascent chain (Supplementary Figure 1a), as expected for a stalled, ribosome-bound translation intermediate [17]. Both the full length and the arrested forms are membrane-integrated, as shown by cell fractionation (Supplementary Figure 1b, c). Induction of synthesis of the arrested form of Lep-SecM(*Ms*), but not of the non-arrested proline-to-alanine mutant, causes accumulation of the precursor form of the SecAYEG-dependent

outer-membrane protein OmpA, Figure 1c, suggesting that arrested Lep-SecM(*Ms*) ribosome-nascent chain complexes block access of pOmpA to SecYEG and hence are stalled in a translocon-bound state.

A pulling force is generated during membrane insertion

By varying *L*, we next mapped the force exerted on the arrest peptide in Lep-SecM(*Ms*) for different locations of the [6L/13A] H segment in the ribosome-translocon-nascent chain conduit. We observed efficient translation arrest except for a region between *L* = 25-45 residues, where the fraction of non-arrested, full length protein (f_{FL}) is dramatically increased, Figure 2a (red curve). The force profile is bi-phasic, with local maxima at *L* ≈ 30 and *L* ≈ 40 residues, indicating a strong pulling force at two distinct stages during translocation. Only marginal increases in f_{FL} were seen for constructs with a less hydrophobic [0L/19A] H segment (brown curve).

To control for possible sequence-specific influences of the linker region between the H segment and the arrest peptide, we made constructs where the linker was shortened from its N-terminal end (blue curve) instead of its C-terminal end (see Supplementary Figure 2a-c). The two force profiles coincide except for *L* = 33-35 and *L* = 42-50 residues, where the C-terminally truncated constructs produce less full length protein. These results imply that the bi-phasic shape of the force profile is determined by the location of the H segment relative to the arrest peptide, and that residues outside the minimal HAPIRGSP arrest peptide can to some extent modulate its overall arrest potency.

The force profile is conserved when 10 residues are deleted in the loop between TM2 and the H segment (Supplementary Figures 2b and 3a), showing that the location of the arrest peptide relative to the TM1-TM2 region is unimportant. Replacement of TM2 by an engineered [8L/11A] segment does not affect f_{FL} at *L* = 39 residues (Supplementary Figure 3a), indicating that f_{FL} is independent of the sequence of TM2. Finally, deletion of the TM1-TM2 region in Lep-SecM(*Ms*) [6L/13A, *L* = 39] to prevent co-translational targeting to the SecYEG translocon [19] results in efficient arrest (Supplementary Figure 3a), demonstrating that the increase in f_{FL} is specific for translocating nascent chains.

Introducing a mutation that is present in a version of the SecM(*Ec*) arrest translation peptide with increased arrest potential (Sup1) [10,16] into SecM(*Ms*) (HPPIRGSP, mutation underlined) results in a force profile where the local maximum at *L* ≈ 30 residues is almost completely suppressed, Figure 2a (black curve); hence, the force exerted on the nascent chain is weaker at *L* ≈ 30 than at *L* ≈ 40. The width of the peak at *L* ≈ 40 is reduced to only 4 residues in Lep-SecM(*Ms*-Sup1), showing that maximal pulling force is exerted only at a precisely defined point during translocation.

We repeated the experiment shown in Figure 2a using the SecM(*Ec*) and the mutant SecM(*Ec*-Sup1) arrest peptides together with the [6L/13A] H segment, Figure 2b (See Supplementary Figure 2d for sequences). The wildtype SecM(*Ec*) arrest peptide has a weaker arrest potential than the SecM(*Ec*-Sup1) and SecM(*Ms*) arrest peptides [10]. The shapes of the force profiles obtained with the SecM(*Ms*) and SecM(*Ec*) wildtype and mutant arrest peptides are qualitatively similar, although the two-peak pattern cannot be resolved with the weaker SecM(*Ec*) wildtype arrest peptide.

To ascertain the generality of the results obtained in *E. coli*, we performed similar experiments in a mammalian *in vitro* translation system supplemented with dog pancreas rough microsomes, using an arrest peptide from the Xbp1 protein [15], Figure 2c and Supplementary Figure 3b. Although the Xbp1 arrest peptide is rather weak, there is a clear maximum in f_{FL} at *L* ≈ 40 residues. Since the Xbp1 arrest peptide itself is 25 residues long

and the GPGG stretch flanking the C-terminal end of the H segment adds another four residues (see Supplementary Figure 2e), we could not study constructs with $L < 29$ and hence cannot say if there is a second peak in the force profile at small L values in this case.

The pulling force increases with H-segment hydrophobicity

What is the relation between pulling force and H-segment hydrophobicity? To address this question, we made Lep-SecM(*Ms*) constructs with H segments of composition [*n*L/(19-*n*)A], and varied n from 0 to 11 while keeping L constant at the local maxima of the force profiles in Figure 2a, i.e., $L = 28$ and 39. For both values of L, f_{FL} increases linearly from background levels for $n \leq 2$ and plateaus at $n \geq 7$, Figure 2d (the block in OmpA export noted in Figure 1c is inversely related to f_{FL} in this experiment, Supplementary Figure 4). By way of comparison, the threshold for 50% insertion of [*n*L/(19-*n*)A] H segments into the inner membrane of *E. coli* is $n \approx 1.5$ [14]. The pulling force on the arrest peptide is therefore apparent only for H segments with membrane-insertion efficiencies > 50%. We performed the same analysis using the SecM(*Ec*) arrest peptide at $L = 39$. The dependency of f_{FL} on n parallels that seen for the SecM(*Ms*) arrest peptide, except that the background level of f_{FL} for $n \leq 2$ is higher, Figure 2d. These results demonstrate that the hydrophobicity of the H segment is the main contributor to the force profiles and imply, together with results reported in Supplementary Figure 5, that SecA is unlikely to have a significant influence.

In order to better understand the molecular interactions responsible for the bi-phasic nature of the force profile, we next introduced either a charged arginine or a helix-breaking proline residue in the N-terminal, middle, or C-terminal part of an H segment of composition [6L/12A/1X] (X = R, P), and analyzed these mutations in Lep-SecM(*Ms*) at the $L = 30$ and $L = 39$ force-profile maxima (Supplementary Figure 6a). At $L = 30$, arginine reduces f_{FL} when placed near the N terminus of the SecM(*Ms*) arrest peptide but has little effect when placed in the middle or near the C terminus, while for $L = 39$, the arginine mutation maximally reduces f_{FL} when placed in the middle but not near the ends of the H segment. This suggest that the local maximum in the force profile at $L = 30$ is caused by a hydrophobic interaction involving the N-terminal end of the H segment, while the maximum at $L = 39$ depends mostly on the hydrophobicity of the H segment's central part. Proline, in contrast, markedly reduces f_{FL} only when placed in the middle of the arrest peptide, both for $L = 30$ and $L = 39$. As proline is a strong helix-breaker [20], the simplest interpretation is that the H segment needs to be in a helical conformation to generate a strong pulling force.

Location of the H segment in the translocon

While it is difficult to determine the precise location of the H segment within the ribosome–translocon conduit in *E. coli* at different values of L, this can be done for the *in vitro*-translated Lep-Xbp1 constructs using glycosylation mapping. This approach rests on the observation that the asparagine residue in an Asn-X-Thr/Ser acceptor site for N-linked glycosylation must be ~15 residues away from the N-terminal end of a membrane-integrated transmembrane H segment to reach the lumenal active site of the oligosaccharyl transferase in the ER and become half-maximally glycosylated [21,22]. We introduced two glycosylation acceptor sites (G1, G2) in the loop between TM2 and the H segment in Lep-Xbp1 [6L/13A], Figure 3a. G1 is sufficiently far away from both TM2 and the H segment to always be glycosylated, and serves as a marker for the lumenal location of the loop. The position of G2 relative to the H segment was varied in order to determine the point of half-maximal glycosylation (the "minimal glycosylation distance", MGD). Translation of Lep-Xbp1 [6L/13A, L=29] yields a mixture of full length and arrested products, Figure 3b, and the amounts of singly and doubly glycosylated chains vary as the G2 site is moved relative to the H segment. From the quantitations shown in Figure 3c, the full length product (red curve) has MGD = 15 (the same value is obtained for a construct with a mutated, non-functional arrest

peptide, black curve and Supplementary Figure 6b), while the arrested product has MGD = 22 (dark blue curve). Truncation of the mRNA after the last codon of the arrest peptide to produce a stalled ribosome-nascent chain translocation intermediate similar to the arrested form also yields MGD = 22 (purple curve and Supplementary Figure 6c). The same truncation of the mRNA encoding Lep-Xbp1 [6L/13A, *L*=41] yields MGD = 16 (light blue curve and Supplementary Figure 6d). Thus, the H segment extends fully into the translocon in Lep-Xbp1 [6L/13A, *L*=41], while in Lep-Xbp1 [6L/13A, *L*=29] its N-terminal end is 22-15 = 7 residues away from the lumenal membrane-water interface, as shown in Figure 3d (II, III). We have found previously that a 65-residue long, extended nascent chain can reach from the ribosomal peptidyl transferase center (PTC) to the active site of the oligosaccharyl transferase [23,24], Figure 3d (IV). For Lep-Xbp1 [6L/13A, *L*=29] and Lep-Xbp1 [6L/13A, *L*=41], the corresponding values are 70 and 76 residues, Figure 3d. Thus, the nascent chain is not fully extended in either construct, most likely because the H segment is at least partly helical.

Discussion

Using two different bacterial and one mammalian arrest peptides as force sensors, we have been able to track forces acting on a nascent chain during the co-translational integration of a transmembrane segment into the inner membrane of *E. coli* and the mammalian ER membrane. From the data presented in Figures 2 and 3, we conclude that a strong, bi-phasic pulling force acts on nascent chains containing a sufficiently hydrophobic H segment, with maxima when the C-terminal end of the H segment is $L \approx 30$ and $L \approx 40$ residues away from the C-terminal residue in the arrest peptide. The force is weaker at $L \approx 30$ than at $L \approx 40$ residues. The force is seen only for [*n*L/(19-*n*)A] H segments for which $n \geq 2$ and is directly proportional to n over the interval $2 < n < 7$. At $L \approx 30$ residues, the force is sensitive to a reduction in the hydrophobicity of the N-terminal but not the middle and C-terminal parts of the H segment, while at $L \approx 40$ residues the middle part is the most critical; in both cases, placing a helix-breaking proline residue in the middle part reduces the force. Finally, at $L \approx 30$ residues, only the N-terminal end of the H segment reaches into the translocon, while at $L \approx 40$ residues the H segment spans the membrane.

The bi-phasic nature of the force profiles suggests that the translocon-to-membrane transition of the H segment proceeds through at least two distinct steps, Figure 4. What could be the nature of these steps? The peak in the force profile at $L \approx 40$ residues likely corresponds to a step where the H segment partitions from the translocon into the surrounding membrane: the H segment extends fully into the translocon at this point; the pulling force increases with the hydrophobicity of the H segment and is reduced by the introduction of a charged arginine residue in center but not near the ends of the H segment (as is the efficiency of membrane insertion [3]); and the pulling force is reduced by the introduction of a central proline residue, suggesting that an α-helical conformation is critical. We estimate that the physical length of the H segment is ~28 Å at this point, corresponding to a 100% α-helical conformation, Figure 3d (III).

The peak at $L \approx 30$ residues corresponds to a situation where only the most N-terminal part of the H segment has entered the translocon channel or is interacting with the lipid surface in the immediate vicinity of the translocon, Figure 3d (II). Consistent with such a location, the introduction of an arginine residue in the N-terminal, but not in the middle or C-terminal, part of the H segment strongly reduces the pulling force. Given its estimated length of ~45 Å, the H segment appears to be ~50% helical. This points to the existence of an early interaction between the H segment and the translocon, distinct from the membrane-integration step.

More generally, our results show that SecM arrest peptides can be used as *in vivo* force sensors to study the behavior of nascent polypeptide chains coming off the ribosome. By varying the strength of the arrest peptide, it is possible to vary the "spring constant" of the force sensor and fine-tune the system to react at different force levels; natural examples of such fine-tuning may be provided by the MifM arrest peptide that monitors YidC-mediated insertion of inner membrane proteins in *Bacillus subtilis* [9] and by the exquisite adaptation between the signal peptide, arrest peptide, and overall chain length recently uncovered for *E. coli* SecM [10]. The approach should be applicable to the study of a range of co-translational processes, including protein folding and interaction of nascent chains with chaperones, molecular motors, and other binding partners.

Online Methods

Enzymes and chemicals

All enzymes were from Fermentas (St. Leon-Rot, Germany), except for *Pfu* Turbo DNA polymerase from Stratagene (La Jolla, CA, USA). Oligonucleotides were from Eurofins MWG Operon (Ebersberg, Germany) and CyberGene (Stockholm, Sweden). L-[^{35}S]-methionine was from PerkinElmer (Waltham, MA, USA). All other reagents were from Sigma-Aldrich (St. Louis, MO, USA).

DNA manipulations

Starting from a previously described pGEM1 plasmid carrying the *lepB* gene with a 6L/13A H segment insert [2], the QuikChange site-directed mutagenesis kit (Promega) was used to introduce a *SacI* restriction site in codons 305-306 of the *lepB* gene and to remove an existing *SacI* site in the vector backbone. Double-stranded oligonucleotides encoding the *E. coli* or *M. succiniciproducens* SecM arrest peptide (and mutant versions thereof) with *SacI* overhangs were introduced into the *SacI* site in the *lepB* gene. The *lepB* coding region was then subcloned into the *NcoI* and *SmaI* sites in the pING1 vector [29,30] to allow expression from an arabinose-inducible promoter. Lep constructs with shorter linker lengths between H3 and the arrest peptide were generated by PCR using forward and reverse primers which were complementary to regions denoted by the right-facing or left-facing arrows respectively in Supplementary Figure 2. The Δ10 constructs were also generated by PCR using a forward primer which starts at codon 175 and a reverse primer which begins from codon 164 of the *lepB* gene. To replace TM2 of Lep with an 8L/11A segment, *ApaI* and *EagI* restriction sites were introduced at codons 55-56 and 78-79 of *lepB* respectively and a PCR-generated fragment encoding the sequence GGPGAAAALALALLLLLALAAAAGPGG was cloned into these sites. Different H segments were introduced into Lep by inserting double-stranded oligonucleotides into *SpeI*/*KpnI* sites as previously described [2]. The control construct shown in Supplementary Figure 3a was generated by a deletion of Lep residues 4-77 and contains Lep residues 305-323 (from the soluble C-terminal Lep domain) in place of the H segment upstream of the SecM arrest peptide. The Lep-Xbp1 construct was generated by a similar fashion. An *Eag*I and a *Sac*I site were introduced into codons 300-301 and 305-306 of the *lepB* gene in the pGEM1 plasmid and double-stranded oligonucleotides coding for the 25-residue Xbp1 arrest peptide were introduced between these sites. Constructs with a non-functional Xbp1 arrest peptide were generated by QuikChange site-directed mutagenesis by the mutation of leucine to arginine in the 25-residue sequence DPVPYQPPFLCQWGRHQPSWKPLMN, where the mutated leucine is underlined. QuikChange site-directed mutagenesis was also used to introduce N-glycosylation acceptor sites, NXT/S, into the indicated locations within Lep-Xbp1 constructs. For the generation of stalled nascent chains, DNA templates used in *in vitro* transcription were generated by PCR using a forward primer complementary to a region ~150 nucleotides upstream of the SP6 promoter, and reverse primers complementary

to either the Xbp1 arrest peptide (for *L*=29, where Lep-Xbp1 *L*=29 coding region was used as the DNA template for PCR), or the *lepB* region which generated *L*=41 (for *L*=41, where Lep-Xbp1 *L*=76 coding region was used as the DNA template).

Pulse-chase analysis

E. coli MC1061 cells [31] carrying the respective *lepB* constructs were grown overnight at 37°C in M9 minimal medium supplemented with 19 amino acids (1 μg ml^{-1}, no Met), 100 μg ml^{-1} thiamine, 0.1 mM $CaCl_2$, 2 mM $MgSO_4$, 0.4% (w/v) fructose and 100 μg ml^{-1} ampicillin. Cultures were then backdiluted 1:10 and grown to OD_{600} = 0.35. Cells were induced for Lep expression with 0.2% (w/v) arabinose for 5 min and pulse-labeled with [^{35}S]-methionine for 2 min at 37°C. Where indicated, a chase was carried out by the addition of 2 mM non-radioactive methionine. Samples were removed at the indicated time points and added to an equal volume of 20% trichloroacetic acid (TCA). After a 30-minute incubation on ice, samples were spun for 5 min at 20,800 g at 4°C. The pellet was washed with cold acetone and the sample was spun again for 5 min at 4°C. The pellet obtained was solubilized in Tris-2%SDS solution (10 mM Tris-Cl pH 7.5, 2% SDS) at 95°C for 10 min and the sample spun for 5 min at room temperature. The SDS-solubilized lysate was then used for immunoprecipitation using Lep and OmpA antisera. The samples were resolved by SDS-PAGE and the gel visualized using a Fuji FLA-3000 phosphoimager and the ImageGauge V4.23 software. Quantification of protein species were performed using the QtiPlot 0.9.7.10 software. All experiments were repeated at least three times.

Cetyltrimethylammonium bromide (CTABr) fractionation

Induction and radio-labeling of cells were carried out as above. TCA-precipitated cell extracts were solubilized in Tris-1%SDS solution (10 mM Tris-Cl pH 7.5, 1% SDS). 500 μl of 2% (w/v) CTABr and 500 μl of 0.5 M sodium acetate pH 4.7 were added to 50 μl of the SDS-solubilized extracts and the samples were placed on ice for 10 min. Samples were then incubated at 30°C for 10 min and spun at full speed in a microfuge for 15 min at room temperature. The pellet was washed once with cold acetone, solubilized in Tris-2%SDS solution and used for immunoprecipitation. The supernatant fraction was first treated with 20% TCA for protein recovery as described above and then processed for immunoprecipitation with Lep antiserum.

Sodium azide treatment

MC1061 cells were cultured and induced for protein expression as described under Pulse-chase analysis above. Sodium azide was added to the indicated final concentrations 1 min after cell induction. After 4 min of azide treatment, the cells were pulse-labeled with [^{35}S]-methionine for 1 min at 37°C and prepared for immunoprecipitation as before. Samples were split into two equal fractions for immunoprecipitation using Lep and OmpA antisera before being resolved by SDS-PAGE.

Cell fractionation

Cells (1.8 ml culture) were induced and labeled as described under Pulse-chase analysis. After 2 min of labeling with [^{35}S]-methionine, 0.5 mg ml^{-1} non-radioactive methionine was added and the cells spun down for 2 min at 20,800 g at 4 °C. All subsequent steps were performed at 4 °C. The cells were resuspended in spheroplast buffer (40% sucrose (w/v), 33 mM Tris, pH 8.0) and converted to spheroplasts by incubation with 1 mM EDTA and 0.1 mg ml^{-1} lysozyme for 30 min. 10 mM $MgSO_4$ was added and the samples were spun for 5 min at 16,600 g. The spheroplasts were resuspended in 50 μl of spheroplast buffer and lysed by the addition of 2 ml of H_2O. Unbroken spheroplasts were removed by centrifugation at 4,500 g for 5 min. 800 μl of the supernatant was TCA-precipitated (designated as totals, T)

and used for immunoprecipitation with Lep or AraB antisera, while the remaining supernatant was separated into cytoplasmic and membrane fractions by centrifugation at 100,000 g for 30 min. The cytoplasmic fraction was TCA-precipitated while the membrane pellet was solubilized in Tris-2%SDS solution before immunoprecipitation.

In vitro transcription and translation

In vitro transcription was performed with SP6 RNA polymerase according to the manufacturer's protocol (Promega) using Lep-XBP1 constructs cloned into the pGEM1 vector for the expression of full length protein, or PCR products as templates for the generation of truncated nascent chains. RNA obtained was purified using RNeasy Mini Kit (Qiagen). Translations were performed in a rabbit reticulocyte lysate system as described (Promega) for 15 min at 30 °C in the presence of 0.5 μl of dog pancreas rough microsomes and 1 μl of [^{35}S] Met (5 μCi). The reaction was stopped by the addition of equal volume of sample buffer and treated with RNase A (200 μg ml^{-1}) for 15 min at 30 °C before the samples were resolved by SDS-PAGE. For puromycin-treated samples, the samples were incubated for an additional 10 min at 30 °C with 1mM puromycin and 5 mM EDTA after translation and sample buffer was added.

Supplementary Material

Refer to Web version on PubMed Central for supplementary material.

Acknowledgments

We thank S. Bhushan, Würzburg, and P. F. Egea, Los Angeles, for advice, and C. Lundin, Stockholm, for technical assistance. This work was supported by grants from the European Research Council (ERC-2008-AdG 232648), the Swedish Foundation for Strategic Research, the Swedish Research Council, and the Swedish Cancer Foundation to GvH.

References

1. White SH, von Heijne G. How translocons select transmembrane helices. Annu Rev Biophys. 2008; 37:23–42. [PubMed: 18573071]
2. Hessa T, et al. Recognition of transmembrane helices by the endoplasmic reticulum translocon. Nature. 2005; 433:377–381. [PubMed: 15674282]
3. Hessa T, et al. Molecular code for transmembrane-helix recognition by the Sec61 translocon. Nature. 2007; 450:1026–1030. [PubMed: 18075582]
4. Schow EV, et al. Arginine in membranes: On the connection between molecular dynamics simulations and translocon-mediated insertion experiments. Mol Membr Biol. 2011; 239:35–48.
5. Ito K, Chiba S, Pogliano K. Divergent stalling sequences sense and control cellular physiology. Biochem Biophys Res Comm. 2010; 393:1–5. [PubMed: 20117091]
6. Sarker S, Rudd KE, Oliver D. Revised translation start site for secM defines an atypical signal peptide that regulates Escherichia coli secA expression. J Bacteriol. 2000; 182:5592–5595. [PubMed: 10986266]
7. Nakatogawa H, Ito K. Secretion monitor, SecM, undergoes self-translation arrest in the cytosol. Mol Cell. 2001; 7:185–192. [PubMed: 11172723]
8. Butkus ME, Prundeanu LB, Oliver DB. Translocon "pulling" of nascent SecM controls the duration of its translational pause and secretion-responsive secA regulation. J Bacteriol. 2003; 185:6719–6722. [PubMed: 14594848]
9. Chiba S, et al. Recruitment of a species-specific translational arrest module to monitor different cellular processes. Proc Natl Acad Sci U S A. 2011; 108:6073–6078. [PubMed: 21383133]
10. Yap MN, Bernstein HD. The translational regulatory function of SecM requires the precise timing of membrane targeting. Mol Microbiol. 2011; 81:540–553. [PubMed: 21635582]

Europe PMC Funders Author Manuscripts

11. Muto H, Nakatogawa H, Ito K. Genetically encoded but nonpolypeptide prolyl-tRNA functions in the A site for SecM-mediated ribosomal stall. Mol Cell. 2006; 22:545–552. [PubMed: 16713584]
12. Garza-Sanchez F, Janssen BD, Hayes CS. Prolyl-tRNA(Pro) in the A-site of SecM-arrested ribosomes inhibits the recruitment of transfer-messenger RNA. J Biol Chem. 2006; 281:34258–34268. [PubMed: 16968693]
13. Gumbart J, Schreiner E, Wilson DN, Beckmann R, Schulten K. Mechanisms of SecM-mediated stalling in the ribosome. Biophys J. 2012; 103:331–341. [PubMed: 22853911]
14. Xie K, et al. Features of transmembrane segments that promote the lateral release from the translocase into the lipid phase. Biochemistry. 2007; 46:15153–15161. [PubMed: 18052199]
15. Yanagitani K, Kimata Y, Kadokura H, Kohno K. Translational pausing ensures membrane targeting and cytoplasmic splicing of XBP1u mRNA. Science. 2011; 331:586–589. [PubMed: 21233347]
16. Yap MN, Bernstein HD. The plasticity of a translation arrest motif yields insights into nascent polypeptide recognition inside the ribosome tunnel. Mol Cell. 2009; 34:201–211. [PubMed: 19394297]
17. Nakatogawa H, Ito K. The ribosomal exit tunnel functions as a discriminating gate. Cell. 2002; 108:629–36. [PubMed: 11893334]
18. San Millan JL, Boyd D, Dalbey R, Wickner W, Beckwith J. Use of PhoA fusions to study the topology of the Escherichia coli inner membrane protein leader peptidase. J Bacteriol. 1989; 171:5536–5541. [PubMed: 2551889]
19. Dalbey RE, Wickner W. Leader peptidase of Escherichia coli: critical role of a small domain in membrane assembly. Science. 1987; 235:783–787. [PubMed: 3544218]
20. Chou PY, Fasman GD. Prediction of Protein Conformation. Biochemistry. 1974; 13:222–245. [PubMed: 4358940]
21. Nilsson I, von Heijne G. Determination of the distance between the oligosaccharyltransferase active site and the endoplasmic reticulum membrane. J Biol Chem. 1993; 268:5798–5801. [PubMed: 8449946]
22. Nilsson I, Whitley P, von Heijne G. The C-terminal ends of internal signal and signal-anchor sequences are positioned differently in the ER translocase. J Cell Biol. 1994; 126:1127–1132. [PubMed: 8063852]
23. Whitley P, Nilsson IM, von Heijne G. A nascent secretory protein may traverse the ribosome/ER translocase complex as an extended chain. J Biol Chem. 1996; 271:6241–6244. [PubMed: 8626416]
24. Mingarro I, Nilsson I, Whitley P, von Heijne G. Different conformations of nascent polypeptides during translocation across the ER membrane. BioMed Central Cell Biol. 2000; 1:3–10. [PubMed: 11178101]
25. Bhushan S, et al. SecM-stalled ribosomes adopt an altered geometry at the peptidyl transferase center. PLoS Biol. 2011; 9:e1000581. [PubMed: 21267063]
26. Menetret JF, et al. The structure of ribosome-channel complexes engaged in protein translocation. Mol Cell. 2000; 6:1219–1232. [PubMed: 11106759]
27. Egea PF, Stroud RM. Lateral opening of a translocon upon entry of protein suggests the mechanism of insertion into membranes. Proc Natl Acad Sci U S A. 2010; 107:17182–17187. [PubMed: 20855604]
28. van den Berg B, et al. X-ray structure of a protein-conducting channel. Nature. 2004; 427:36–44. [PubMed: 14661030]
29. Johnston S, Lee JH, Ray DS. High-level expression of M13 gene II protein from an inducible polycistronic messenger RNA. Gene. 1985; 34:137–145. [PubMed: 4007491]
30. Dalbey RE, Wickner W. Leader peptidase catalyzes the release of exported proteins from the outer surface of the Escherichia coli plasma membrane. J Biol Chem. 1985; 260:15925–15931. [PubMed: 2999144]
31. Dalbey RE, Wickner W. The role of the polar, carboxyl-terminal domain of Escherichia coli leader peptidase in its translocation across the plasma membrane. J Biol Chem. 1986; 261:13844–13849. [PubMed: 3531212]

Europe PMC Funders Author Manuscripts

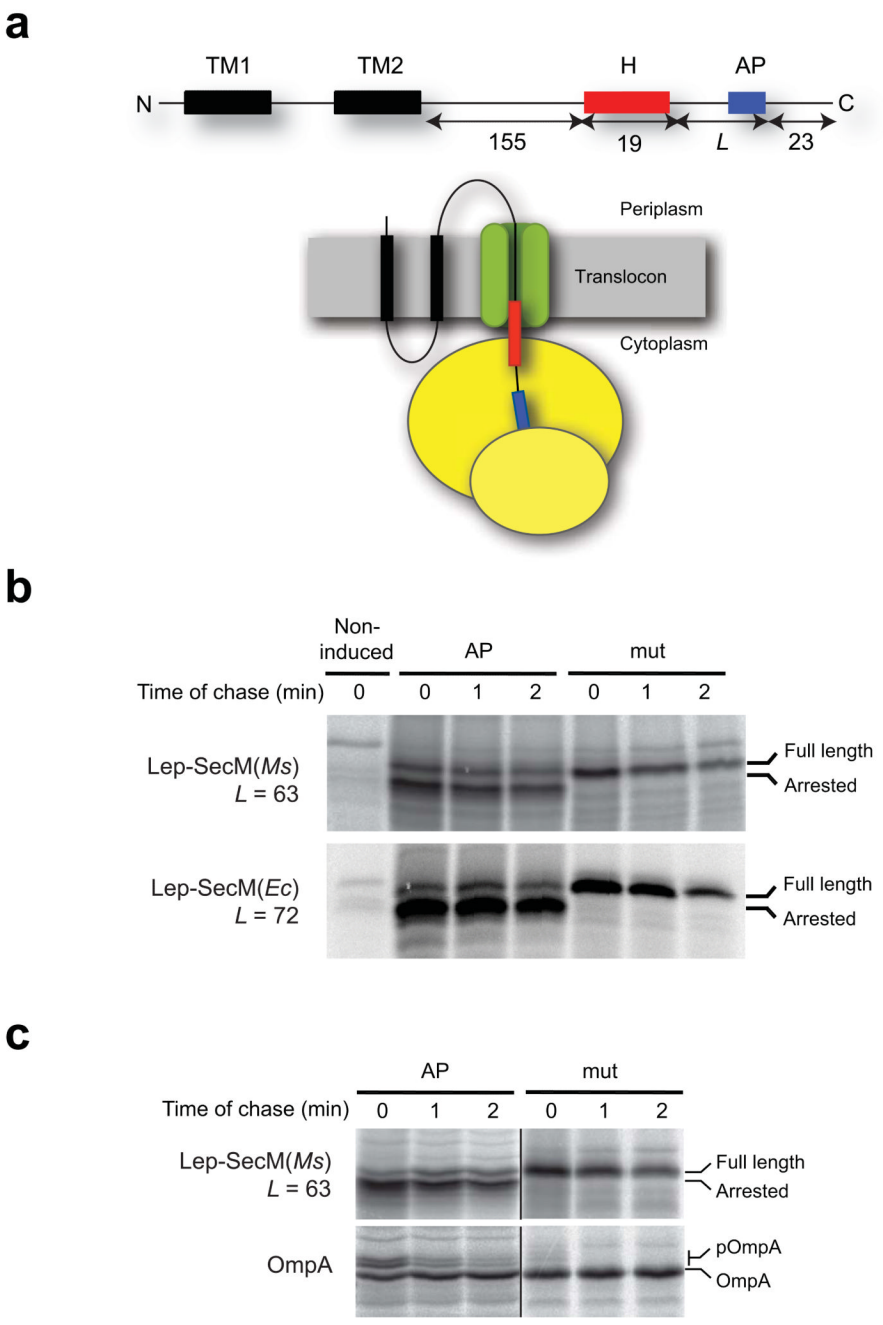

Figure 1.

Translation arrest of Lep constructs induced by the *M. succiniciproducens* and *E. coli* SecM arrest peptides. (**a**) Design of Lep constructs, with the 19-residue long H segment in red and the arrest peptide (AP) in blue. A schematic picture of a translating ribosome bound to the SecYEG translocon is shown below. (**b**) Pulse-chase analysis of constructs with a transmembrane H segment of composition [6L/13A] and *L* = 63 (*Ms*) or *L* = 72 (*Ec*) residues. Constructs with a functional or a mutant, non-functional arrest peptide are denoted AP and mut, respectively. [^{35}S]-methionine labeled protein was precipitated using a Lep antiserum. (**c**) Pulse-chase analysis of the conversion of the precursor form (pOmpA) to the

mature form of OmpA during expression of the indicated Lep-SecM(*Ms*) constructs. [^{35}S]-methionine labeled protein was precipitated using either Lep or OmpA antiserum.

Europe PMC Funders Author Manuscripts

Europe PMC Funders Author Manuscripts

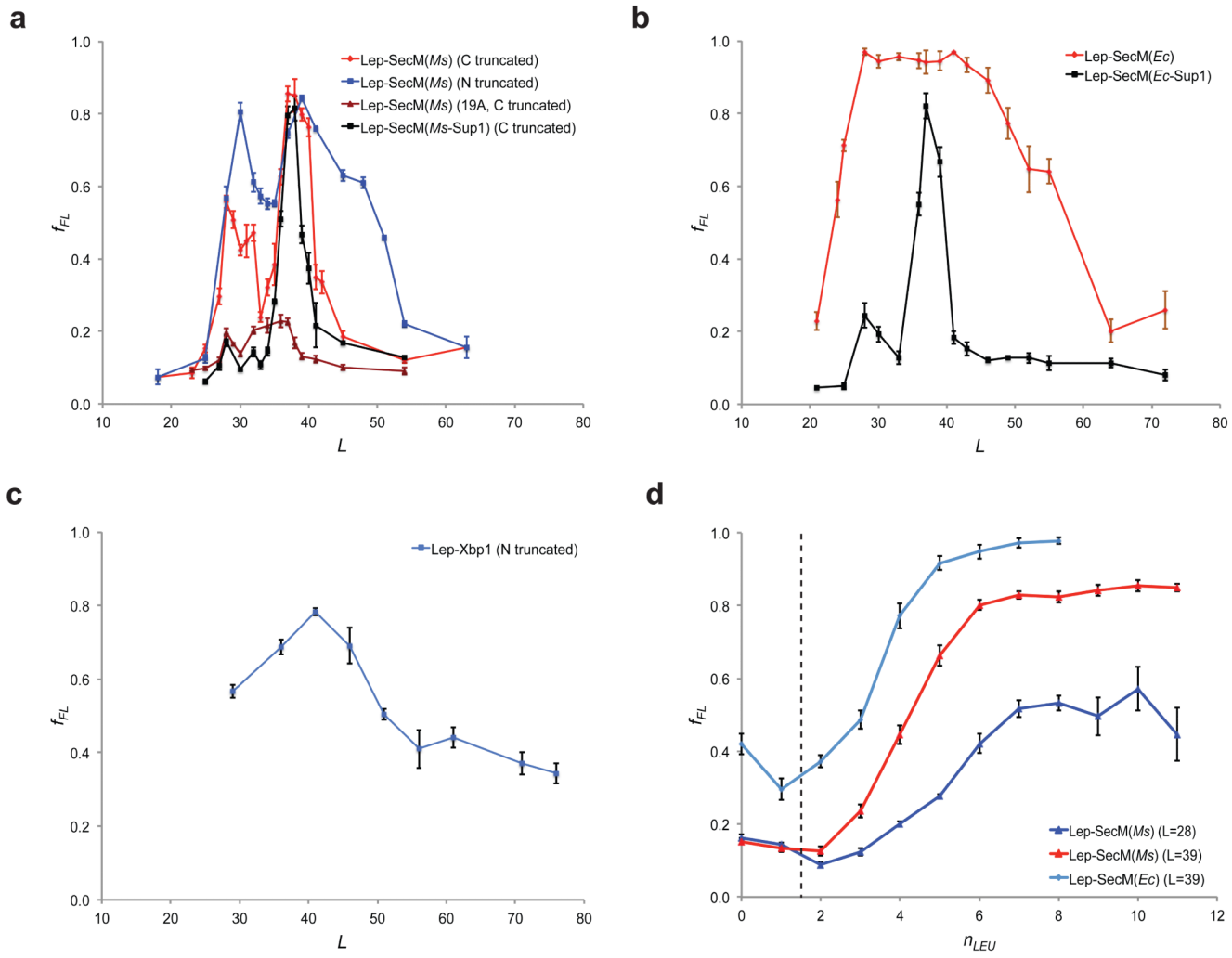

Figure 2.

A bi-phasic pulling force acts on the nascent chain. (**a**) Fraction of full length molecules f_{FL} after a 2 min. pulse with [^{35}S] methionine plotted as a function of L for Lep-SecM(*Ms*) [6L/13A] constructs truncated from either the C-terminal end (C truncated; red curve) or the N-terminal end (N truncated; blue curve) of the linker between the H segment and the arrest peptide. f_{FL} values for Lep-SecM(*Ms*-Sup1) (6L/13A, C truncated) constructs (black curve) and Lep-SecM(*Ms*) (19A, C truncated) constructs (brown curve) are also shown. (**b**) Same as in (a), but for Lep-SecM(*Ec*) (6L/13A, C truncated) constructs (red curve), and Lep-SecM(*Ec*-Sup1) (6L/13A, C truncated) constructs (black curve). (**c**) f_{FL} plotted as a function of L for Lep-Xbp1 (6L/13A, N truncated) constructs translated *in vitro* in the presence of dog pancreas rough microsomes. The sequences of constructs used in (a) to (c) can be found in Supplementary Figure 2. (**d**) f_{FL} for Lep-SecM(*Ms*) (C truncated, L=28, 39) constructs (blue and red curves) and Lep-SecM(*Ec*) (C truncated, L=39) constructs (light blue curve) plotted as a function of the number of leucine residues (n) for H segments of the composition nL/(19-n)A. The dashed line indicates the threshold for 50% membrane insertion of the H segment. Error bars indicate ±1 SEM in all panels.

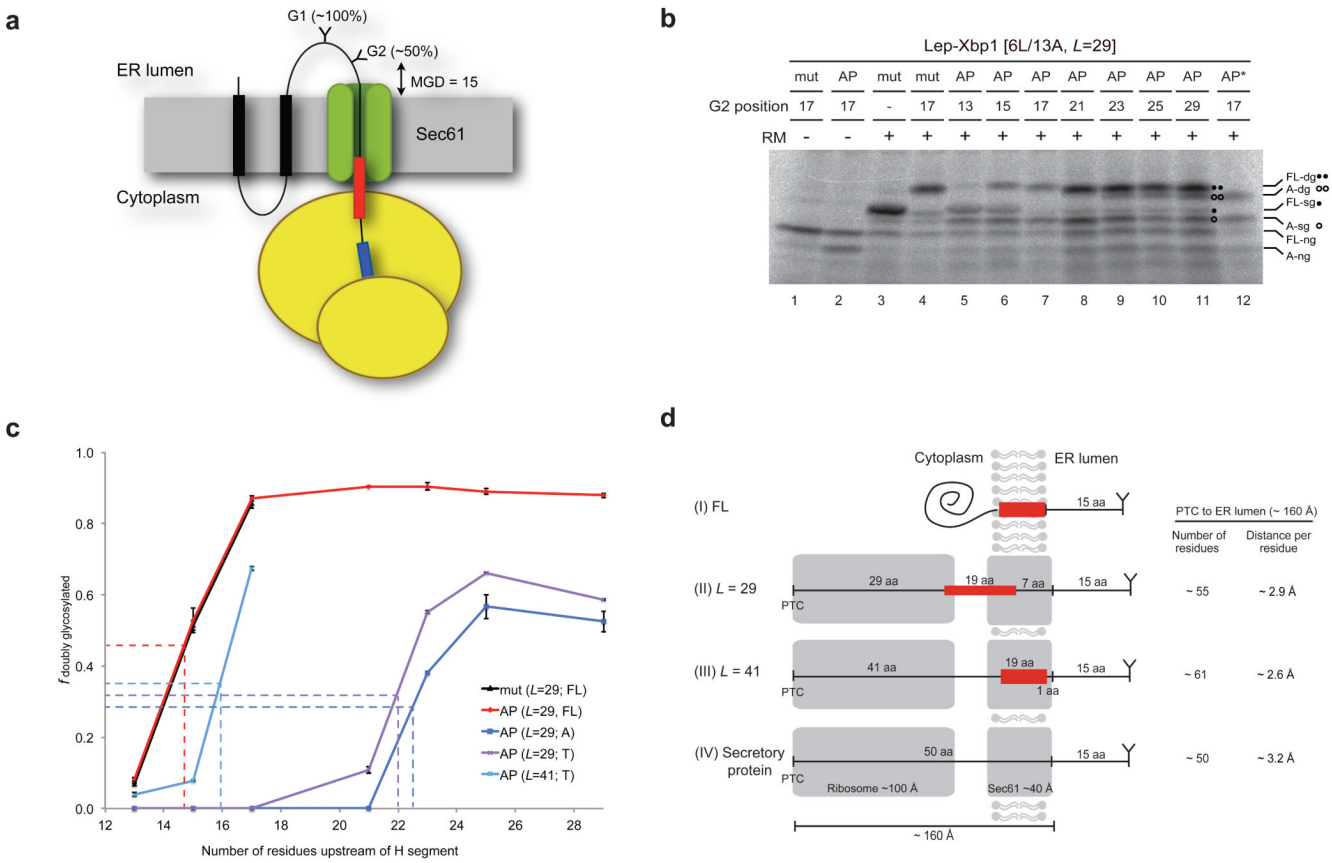

Figure 3.

Determination of the location of the H segment in the translocon by glycosylation mapping. (**a**) Schematic diagram indicating the locations of the two N-glycosylation sites (G1 and G2) in the Lep-Xbp1 constructs. (**b**) *In vitro* translation of Lep-Xbp1 [6L/13A, L=29] constructs in the presence (+RM) and absence (-RM) of dog pancreas rough microsomes. The number of residues between the asparagine in the G2 site and the N-terminal end of the H segment is indicated above each lane. Constructs with a functional or a non-functional arrest peptide are denoted AP and mut, respectively. FL: Full length chains, A: arrested chains. Non-glycosylated, singly glycosylated and doubly glycosylated chains are denoted ng, sg, and dg, respectively. Constructs with a non-functional arrest peptide without a G2 site (lane 3) or, with a G2 site at position 17 (lane 4), were used as markers for singly glycosylated and doubly glycosylated full length species respectively. A construct with a G2 site at position 17 and a stop codon after the arrest peptide (AP*) served as a marker for both singly and doubly glycosylated arrested species (lane 12). (**c**) Fraction of doubly glycosylated species plotted as a function of the number of residues between the G2 site and the H segment for full length (FL) and arrested (A) chains of Lep-Xbp1 [6L/13A, *L*=29] constructs with functional (AP) or non-functional (mut) arrest peptide, and of nascent chains generated by translation of Lep-Xbp1 [6L/13A] mRNAs truncated at *L*=29 and *L*=41 (T). (**d**) Schematic diagram showing estimates of the location of the H segment in the ribosome-translocon-nascent chain conduit for *L* = 29 and *L* = 41. The distance between the ribosomal peptidyl transferase center (PTC) and the tunnel exit is ~100 Å [25,26] and a gap of ~20 Å is present between the ribosomal exit tunnel and the SecYEG translocon channel [27]. The translocon channel itself is estimated to be ~40 Å long [28], giving a total distance of ~160 Å from the PTC to the lumenal interface of the ER membrane.

Europe PMC Funders Author Manuscripts

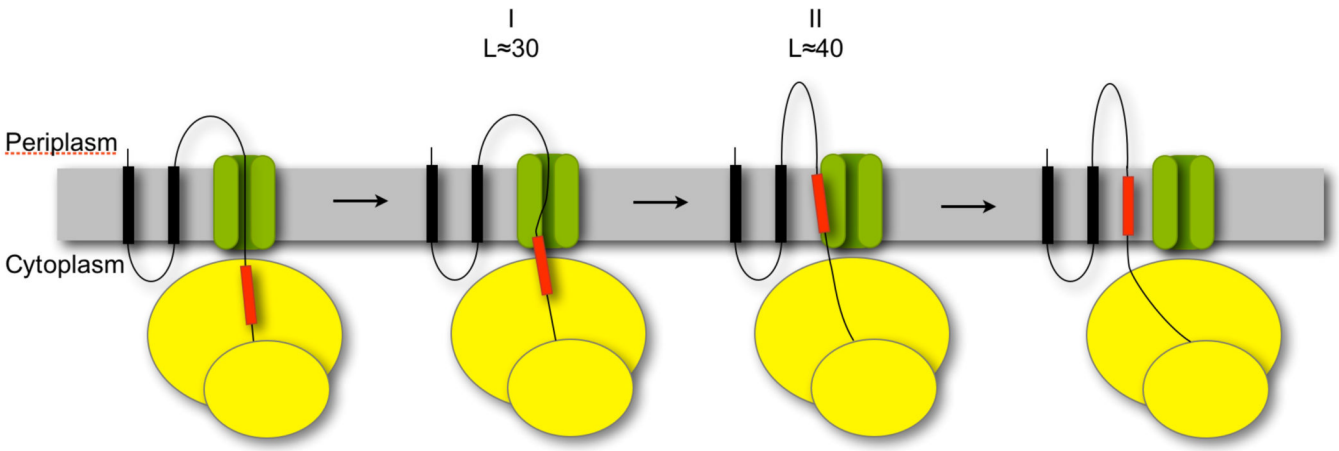

Figure 4.
Model for membrane integration. A strong pulling force is exerted on the nascent chain during the brief moments when the transmembrane helix (red) reaches the translocon channel (I) and when it partitions from the transclocon into the surrounding lipid (II).

Europe PMC Funders Author Manuscripts